universe

MDPI

Review

Revealing Neutrino Oscillations Unknowns with Reactor and Long-Baseline Accelerator Experiments

Inés Gil-Botella *,† and Carmen Palomares *,†

Centro de Investigaciones Energéticas, Medioambientales y Tecnológicas (CIEMAT), 28040 Madrid, Spain
* Correspondence: ines.gil@ciemat.es (I.G.-B.); mc.palomares@ciemat.es (C.P.)
† These authors contributed equally to this work.

Abstract: Reactor and accelerator-based neutrino experiments have played a critical role in the understanding of neutrino oscillations and are currently dominating the high-precision measurements of neutrino oscillation parameters. The discovery of a non-zero θ_{13} by the reactor experiments has opened the possibility of observing CP violation in the lepton sector by long-baseline accelerator experiments. The current knowledge of the neutrino oscillation parameters will be expanded upon in the near future through more precise measurements, including the discovery of the neutrino mass ordering and the CP-violating phase. This review summarizes the distinct and complementary approach of reactor and accelerator-based neutrino experiments to measure neutrino oscillations. The main scientific achievements of the Double Chooz reactor neutrino experiment and the science program to be developed by the DUNE long-baseline neutrino experiment with the world's most intense neutrino beam are presented in this article. Spain has strongly contributed to these results and will continue to play a prominent role in the neutrino oscillation program in the coming years.

Keywords: neutrino physics; neutrino oscillations; reactor neutrinos; accelerator neutrinos; liquid argon TPC

Citation: Gil-Botella, I.; Palomares, C. Revealing Neutrino Oscillations Unknowns with Reactor and Long-Baseline Accelerator Experiments. *Universe* **2022**, *8*, 81. https://doi.org/10.3390/universe8020081

Academic Editors: Susana Cebrian Guajardo, María Martínez Pérez and Carlos Peña Garay

Received: 23 December 2021
Accepted: 22 January 2022
Published: 27 January 2022

1. Introduction

Neutrino physics is one of the fundamental areas in particle physics, with a big impact on astroparticle physics and cosmology, which is still to be explored. In the latest years, great improvements in the experimental field have contributed to understand the neutrino oscillation phenomenon. This is only possible if neutrinos are massive, which is the first indication of new physics beyond the standard model of particle physics.

Neutrino oscillations consist of the transformation in flight from one neutrino flavor to another. In the simplest neutrino scenario, this mechanism is described by two mass squared differences (Δm^2_{21}, Δm^2_{32}) and by the PMNS mixing matrix (analogous to the CKM matrix of the quark sector), which contains three angles (θ_{12}, θ_{23}, θ_{13}) and one CP-violating phase, δ_{CP}. The PMNS matrix establishes the connection between the "flavor" neutrino states (that suffer weak interactions) and the "mass" states (with defined mass values) governing their transformations in flight. In 2015, Profs. T. Kajita and A.B. McDonald were awarded the Nobel prize in physics for the discovery of the neutrino mass through neutrino oscillations.

Solar, reactor, atmospheric and accelerator neutrino experiments have measured with precision the three mixing angles θ_{23}, θ_{12} and θ_{13} and the mass differences $|\Delta m^2_{32}|$ and Δm^2_{21}. There are two possible mass orderings (MO) for neutrinos, according to the positive or negative sign of Δm^2_{32}, referred to as normal ordering (NO) or inverted ordering (IO), respectively.

Table 1 summarizes the results from the frequentist global fit to neutrino oscillation data from reference [1]. The precise values of δ_{CP}, the octant of θ_{23} and the ordering of the neutrino mass spectrum remain still unknown.

Table 1. Determination of the three-flavour neutrino oscillation parameters from a global fit to current neutrino oscillation measurements [1].

Parameter	Best Fit $\pm$ 1σ	3σ Range
Δm^2_{21} [10^{-5} eV^2]	$7.50^{+0.22}_{-0.20}$	6.94–8.14
$\lvert\Delta m^2_{31}\rvert$ [10^{-3} eV^2] (NO)	$2.55^{+0.02}_{-0.03}$	2.47–2.63
$\lvert\Delta m^2_{31}\rvert$ [10^{-3} eV^2] (IO)	$2.45^{+0.02}_{-0.03}$	2.37–2.53
$\sin^2\theta_{12}/10^{-1}$	3.18 ± 0.16	2.71–3.69
$\sin^2\theta_{23}/10^{-1}$ (NO)	5.74 ± 0.14	4.34–6.10
$\sin^2\theta_{23}/10^{-1}$ (IO)	$5.78^{+0.10}_{-0.17}$	4.33–6.08
$\sin^2\theta_{13}/10^{-2}$ (NO)	$2.200^{+0.069}_{-0.062}$	2.000–2.405
$\sin^2\theta_{13}/10^{-2}$ (IO)	$2.225^{+0.064}_{-0.070}$	2.018–2.424
$\delta_{CP}/^\circ$ (NO)	194^{+24}_{-22}	128–359
$\delta_{CP}/^\circ$ (IO)	284^{+26}_{-28}	200–353

The interplay between reactor and accelerator-based neutrino experiments has been crucial to improve our knowledge of the neutrino oscillations. Short-baseline reactor and accelerator neutrino experiments are of huge importance in the era of neutrino oscillation precision measurements. The precise determination of θ_{23}, and the measurements of δ_{CP} and neutrino mass ordering by long-baseline accelerator experiments could provide insight into models behind neutrino mass and lepton mixing. The very precise reactor determination of θ_{13} can result on an improvement of the accelerator experiments sensitivity to δ_{CP}. On the other hand, consistent measurements of θ_{13} would support the three-flavor model of neutrino oscillations.

In this article we review the role of reactor and accelerator neutrino experiments in the determination of the neutrino oscillation parameters. In particular, the Double Chooz reactor neutrino and the DUNE long-baseline neutrino experiments are described in detail. The main results and contributions of Spain to these projects are also summarized.

2. Reactor Neutrino Experiments

Nuclear reactors are very intense sources of neutrinos in the MeV energy region that have been used from its discovery up to the recent precision measurement of θ_{13}. About 2×10^{20} ν/s are emitted in a 4π solid angle from a reactor of 1 GW thermal power. They are produced by the β-decay of the reactor fission products. The neutrino flux is in fact pure electronic antineutrinos ($\bar{\nu}_e$) because all decays of unstable fission products, which are neutron-rich nuclei, are the β-type. The antineutrino flux depends on the reactor thermal power and, for the four main fissioning isotopes, ^{235}U, ^{239}Pu, ^{238}U, and ^{241}Pu, on their fraction of the total fuel content, their energy released per fission, and their fission and capture cross-sections. There are two main methods to compute the reactor antineutrino energy spectra. The first one uses the nuclear databases information of each fission fragment and its decays with the so-called summation technique. The second model relies on the conversion of cumulative electron spectra associated with the beta decays of fission fragments. The reference antineutrino spectra for the main fissible isotope are derived from the measurements of the β spectra at the Institut Laue–Langevin (ILL) research reactor in Grenoble, France, in the 1980s [2,3]. In the case of ^{238}U, an ab initio calculation of the spectrum is often used [4]; more recently, a new measurement of the spectrum from ^{238}U [5] has also been used. The conversion of the β spectra to antineutrino spectra has been improved by using more data on the many β transitions and higher-order energy corrections [4,6].

Electron antineutrino disappearance is the only channel to study neutrino oscillations with reactor experiments because the $\bar{\nu}_e$ energy is not sufficient to produce heavier charged leptons via charge current interactions from $\bar{\nu}_\mu$ or $\bar{\nu}_\tau$. Reactor antineutrinos are observed using the inverse β-decay (IBD) reaction $\bar{\nu}_e + p \rightarrow e^+ + n$, in which there is a positron whose signal is promptly seen. The background is efficiently suppressed thanks to the

coincidence with the delayed signal from γ rays emitted by the neutron capture on nucleus. The energy deposited by the positron, including annihilation, is related to antineutrino energy $E_{\bar{\nu}_e}$ by $E_{prompt} = E_{\bar{\nu}_e} - T_n + 0.8$ MeV where T_n denotes the average neutron recoil energy and is small compared to $E_{\bar{\nu}_e}$. Detectors based on hydrocarbon liquid scintillators provide the free proton targets. The neutron detection efficiency can be increased by loading the liquid scintillator with gadolinium. Gadolinium has a large neutron capture cross section and the emitted γ rays have higher energy, of about 8 MeV, than the 2.2 MeV for the capture by hydrogen.

The study of neutrino oscillation at a reactor is based on the measurement of the $\bar{\nu}_e$ disappearance. A deficit of neutrinos of energy E at a distance L can be interpreted in terms of the survival probability. Experiments with O(100) km baseline are sensitive to Δm^2_{21} (like KamLAND [7]), while ∼1 km of baseline results in a sensitivity to Δm^2_{32} and to θ_{13}. Reactor neutrino experiments provide the most precise measurement of θ_{13} being unaffected by correlations or degeneracies between other parameters. In the two flavors scheme, the survival probability is expressed as:

$$P(\bar{\nu}_e \rightarrow \bar{\nu}_e) \approx 1 - \sin^2 2\theta_{13} \sin^2 \left(\frac{1.27 \Delta m^2_{32}(\mathrm{eV}^2) L(\mathrm{m})}{E(\mathrm{MeV})} \right)$$

This equation is a good approximation to reactor neutrino oscillations even in matter for L less than a few km. θ_{13} can be directly measured from the oscillation amplitude inferred from an energy-dependent deficit in the number of observed neutrinos. To be sensitive to the small value of this parameter, experiments with two identical detectors are mandatory to reduce systematic uncertainties. Three reactor θ_{13} experiments have been realized: Double Chooz in France [8], Daya Bay in China [9], and RENO in Korea [10]. These three experiments employ similar detector design optimized for the precise measurement of reactor antineutrinos.

2.1. Double Chooz

The Double Chooz (DC) experiment is located at the Chooz nuclear power plant in France, having two cores yielding a total thermal power of 8.54 GWth. The DC far detector (FD) is located ∼1050 m from the cores, close to the first oscillation maximum and under 300 m.w.e. rock overburden. The DC FD took data from April 2011 to December 2017. A second identical detector (near detector ND) is placed 400 m away from the reactor cores, in a new laboratory (115 m.w.e.) and operated since December 2014 until the end of 2017. The θ_{13} signature manifests itself as a rate deficit with an up to 10% spectral distortion in the FD relative to the almost undistorted ND spectrum.This two-detector layout, with an almost iso-flux geometry (the fraction of flux from the two reactors is the same in both detectors), allows one to drastically reduce the systematic errors associated with the neutrino flux and detection uncertainties.

The DC detector system is shown in Figure 1. The main bulk of the detector is made of four concentric cylindrical tanks with three central volumes optically coupled. The innermost volume (target) contains 10.3 m^3 of Gd-loaded (1 g/L) liquid scintillator inside a transparent acrylic vessel, where the neutrinos interact via the IBD process. The target is surrounded by three cylindrical layers. A Gd-free liquid scintillator layer, Gamma-Catcher (GC), in a second acrylic vessel is used to detect γ-rays escaping from the target. A mineral oil layer, buffer, works as a shield from radioactivity coming from photomultipliers and the surrounding rock. The 390 low background 10-inch photomultipliers (PMTs) are installed on the inner wall of a stainless steel buffer tank to collect the scintillation light from the inner volumes. The last cylinder is a liquid scintillator layer, inner veto, equipped with 78 8-inch PMTs, that works as cosmic ray muon veto. The whole detector is further surrounded by a 15 cm thick steel shield in the case of the FD and by 1m water tank in the case of the ND to protect it against external γ-rays. The upper part of the detector is covered by an outer muon veto system (OV) consisting of plastic scintillator strips modules to tag muons.

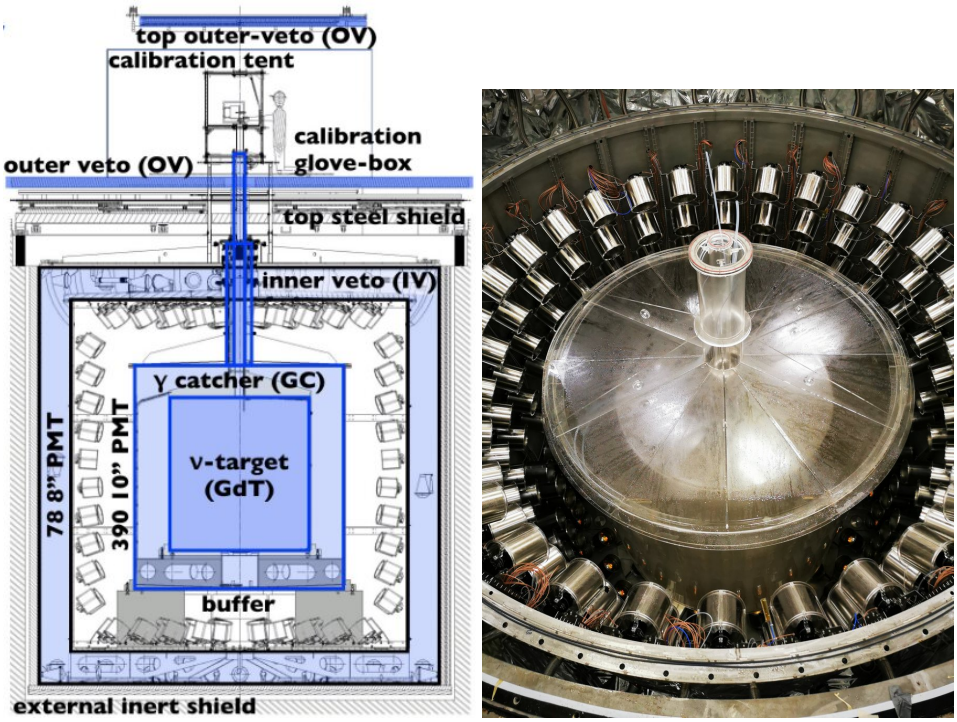

Figure 1. (**Left**): A cross-sectional view of one of the two identical detectors of Double Chooz. (**Right**): A picture of the near inner detector where the target and GC acrylic vessels and the photo-multipliers (with their individual magnetic shielding) are visible.

DC started the data gathering with the far detector in April 2011 and presented its first results in November 2011 with 15.34 GW-ton-years of exposure. DC provided the first indication of a non-zero value of θ_{13} by a reactor-based experiment ($\sin^2(2\theta_{13}) = 0.086 \pm 0.041$) [11]. Since then, many efforts and advances have been performed by the collaboration to improve this result, using the data with the FD while the ND was under construction. Updated analyses on θ_{13} were published in 2012 [12] and 2014 [13] with additional data and a better energy reconstruction, additional muon vetos and novel techniques to achieve significant reductions in the backgrounds and systematic uncertainties.

The last published θ_{13} analysis includes 384 days of data with both detectors FD and ND [14]. The inclusion of an identical ND reduces the neutrino flux uncertainty at the necessary low level, mitigating any possible impact of the reactor model prediction on the θ_{13} measurement. This last result supersedes the previous DC θ_{13} measurements with a value of $\sin^2(2\theta_{13}) = 0.105 \pm 0.014$.

2.2. The Measurement of the θ_{13} Mixing Angle

In addition to reactor experiments, neutrino beam experiments, such as T2K [15] and NOvA [16], are also sensitive to θ_{13} via the appearance $\nu_\mu \rightarrow \nu_e$ and $\bar{\nu}_\mu \rightarrow \bar{\nu}_e$ oscillation modes. However, their measurement of θ_{13} is limited by uncertainties and unknowns such as the δ_{CP} and θ_{23} octant degeneracy. Today's world best value [1] is driven by the statistical combination of the latest θ_{13} published results from reactor experiments [14,17,18]. All θ_{13} reactor experiments are cross-validating each other, which is critical to ensure a robust and unambiguous result.

Double Chooz provided clean analysis results by using unique techniques such as the exploitation of the effective iso-flux site geometry which cancels possible difference between the two reactors, a model-independent background estimation via reactor power modulation including reactor-off data and the total neutron capture detection technique which significantly increases the neutrino event statistics.

The simple Chooz site geometry enabled the placement of the ND at a position relative to the two reactors and the FD in such a way that both, ND and FD, are exposed to both

reactors with the same fraction. This iso-flux position implies that the neutrino fluxes from the two reactors are expected to be largely correlated across detectors, with negligible impact from reactor power or composition variations. This correlation translates into an almost total flux-error cancellation [8,19], a unique DC feature as compared to other reactor θ_{13} experiments [20]. The ND becomes a direct reactor monitor of the FD.

As explained before, the $\bar{\nu}_e$ is detected via the IBD interaction on free protons through the coincidence of the prompt e^+ signal and the delayed neutron capture several μs later. Gd's high n-capture probability reduces the mean capture time from ∼200 μs in metal-free organic liquid scintillator to ∼30 μs. The total neutron capture detection technique used by DC in its two-detector analysis relies on a larger delayed energy range integrating over the γ-peaks of all capturing elements available, H-n, C-n and Gd-n (shown in Figure 2). The IBD space-time coincidence definition relies on a multi-variable artificial neural network thus rejecting uncorrelated background coincidences. More than two orders of magnitude of accidental background rejection is possible while keeping a high average selection efficiency of 86.78 ± 0.21% and 85.47 ± 0.08% for the FD and ND, respectively. In this way, the detection volume expands to both the neutrino target volume loaded with Gd and the gamma-catcher, so the neutrino interaction volume increases a factor ∼3 as compared to Gd only. This increase in statistics is critical for the DC sensitivity.

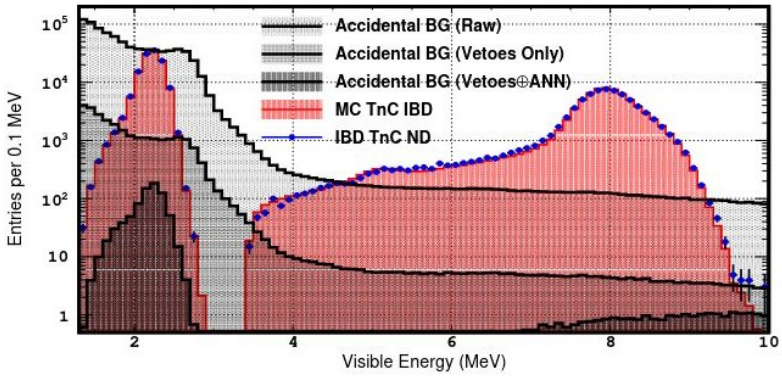

Figure 2. Energy of the delayed signal. The deposited energy by γ's from the neutron capture: ∼2.2 MeV (H-n), ∼5.0 MeV (C-n) and ∼8 MeV (Gd-n) is shown in red. The accidental background (grey histogram) is rejected over more than 4 orders of magnitude below 3.5 MeV using vetoes and the neural network (ANN) selection. An excellent data (blue points) to MC (red area) agreement is found in the delayed energy distribution after the rejection [14].

The θ_{13} measurement is obtained by contrasting the observed IBD rate and shape spectral distortion against the specific neutrino oscillation model prediction obtained with dedicated Monte-Carlo (MC) simulations. The rate and spectrum shape fit uses all detectors data simultaneously. The nominal fit considers the input from each detector fit (data to its MC), as shown in Figure 3, including pertinent constraints and inter-detector correlations such as expected background shape, detection rate, energy spectra and flux. The best fit value is $\sin^2(2\theta_{13}) = 0.105 \pm 0.014$ [14].

Two dominant spectral distortions can be appreciated in Figure 3: the θ_{13} signature (mainly FD) and a common 5 MeV excess, leading to a large χ^2/DoF of 182/112 since the distortions are not covered by the model uncertainties. The FD to ND data ratio (Figure 4(left)) represents a clean θ_{13} rate+shape disappearance evidence. No traces of any remaining distortion are found.

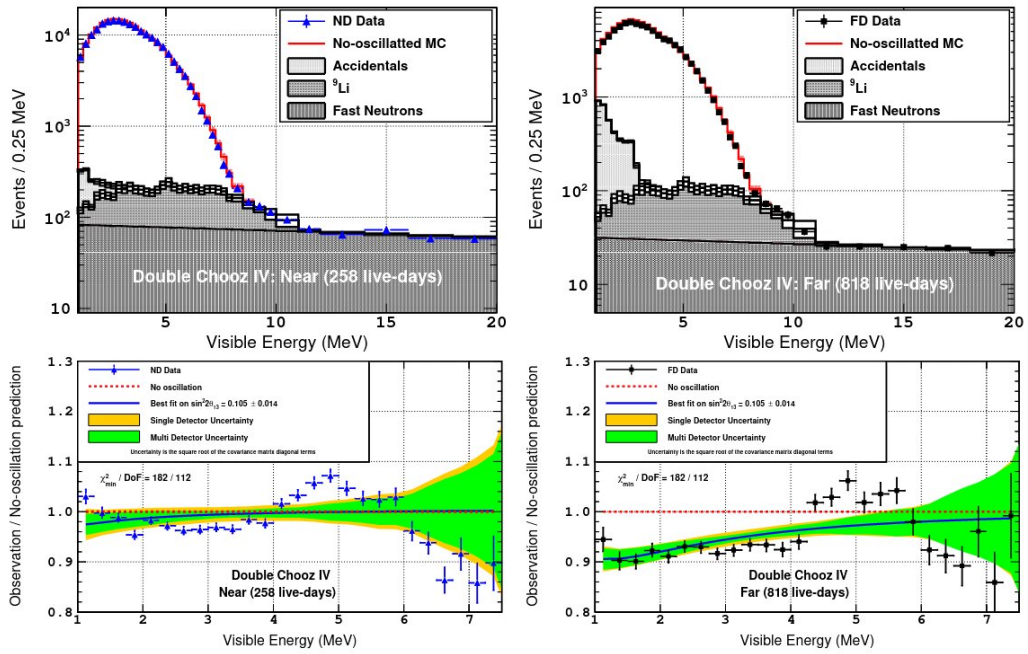

Figure 3. ND (**left**) and FD (**right**) spectra and single-detector ratios. Both ND and FD spectra are shown in the top plots, including the un-oscillated MC prediction (red) and the background model: accidentals (clear grey), ^{9}Li (grey) and fast-neutron (dark grey). The data (background subtracted) to prediction ratio is shown in the bottom panels [14].

Reactor-θ_{13} experiments spectra and the reactor flux model exhibit a significant discrepancy around ∼5 MeV, as illustrated in Figure 4(right). The 5 MeV excess was first published by DC in 2014 [13]. Confirmations by RENO and Daya Bay were reported shortly after. This distortion scales with reactor power; so, an unknown new background hypothesis is ruled out. An inaccurate reactor model prediction is the most appealing hypothesis; other hypotheses have also been suggested [21].

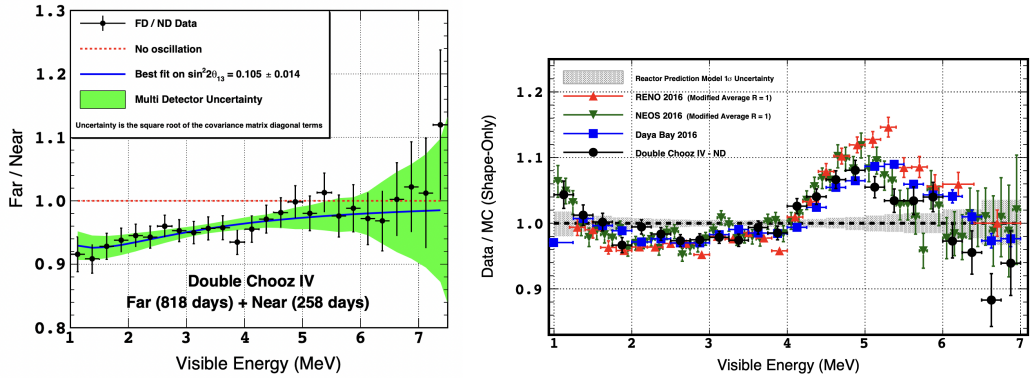

Figure 4. (**Left**): The FD to ND data ratio where the θ_{13} disappearance pattern is observed. (**Right**): The data to prediction spectral ratio for the latest DC-ND [14] (black), Daya Bay [22] (blue), RENO [23] (red), NEOS [24] (green) are shown, exhibiting a common dominant pattern predominantly characterised by the 5 MeV excess. The reactor model prediction shape-only uncertainty is shown in grey [14].

The latest published values of θ_{13} are shown in Figure 5. The results of Double Chooz, Daya Bay and RENO reactor are consistent within systematic uncertainties. The three θ_{13} reactor experiments have already finished their data taking and, hence, their θ_{13} measurements will be the most precise ones for decades. Considering the degeneracies and correlations among oscillation parameters governing the ν_e appearance probability in

long-baseline experiments, the θ_{13} precise measurement of reactor experiments becomes essential to obtain reliable results for δ_{CP}.

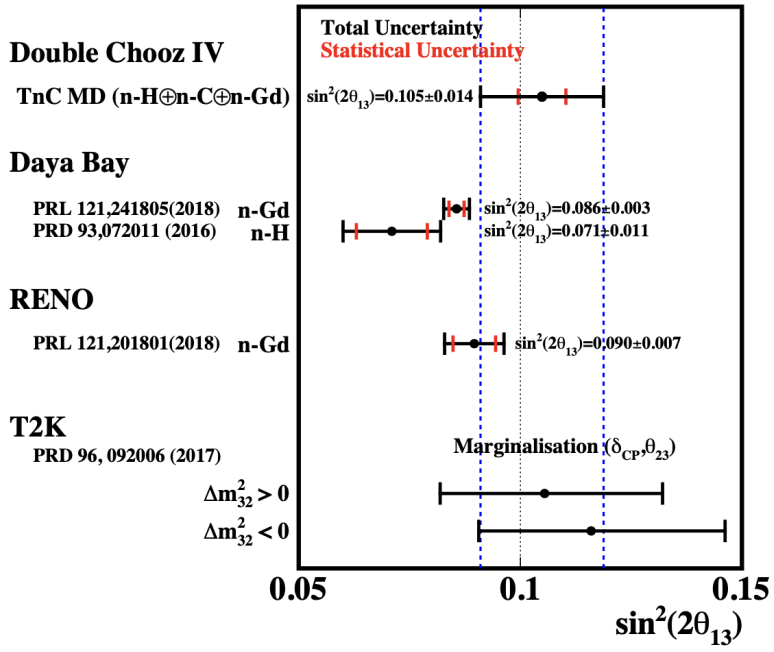

Figure 5. Latest published θ_{13} measurements.

2.3. Spanish Contribution to Double Chooz

The CIEMAT neutrino group has been a member of the Double Chooz collaboration since March 2006. This group has strongly contributed to the DC experiment in both hardware and detector construction and physics data analysis. The CIEMAT group has participated very actively in the DC experiment, assuming important responsibilities in the far and near detector construction [25–27], and making critical contributions to the measurement of θ_{13}.

A second independent measurement of θ_{13} was performed by DC using a different analysis technique led by the Spanish group: the reactor rate modulation (RRM) analysis. The rate of neutrino candidates was measured during periods of different reactor power ranging from zero power (reactor-off) to full power. This analysis allows the measurement of θ_{13} without an a priori knowledge of the background [28] and independently of the spectral distortion [29]. The RRM method is unique to DC because of its simpler site layout. The Chooz total reactor power modulation allows for 2-reactors on, 1-reactor on (either) and the unique background-only data set when both reactors are off. An exposure of $\sim$25 days of reactor-off data allows the measurement of the irreducible background. The background-model-independent method yields $\sin^2(2\theta_{13}) = 0.094 \pm 0.017$ [30]. In the same fit, the total background rates are also obtained, being fully consistent with the cosmogenic background model considered in the rate+shape analysis.

The CIEMAT group is also responsible of the accidental background estimation. The accidental coincidences are the main backgound in the energy region where the neutrino oscillation is maximum. The integration over all n-capture γ's reduces the background rejection capability of the Gd n-capture analysis, increasing the accidental background a factor 40. However, the estimation method developed by the CIEMAT group [31] makes their impact to the θ_{13} measurement negligible, being measured with a precision $<$0.5%.

The CIEMAT group was also in charge of the selection systematics estimation, for which an IBD data-driven inclusive approach was developed [32,33]. The estimator simultaneously integrates over the IBD spectrum in the whole volume, the neural network selection correlations and dependencies and the energy scale systematics including uniformity, stability and linearity, taking into account correlations among all the above terms.

The robustness of the IBD-based methodology was demonstrated with two methods using independent data: ^{252}Cf data sampling using only Gd n-capture events and fast-neutrons data. Agreement across ND and FD is within 0.1%. Thus, the uncertainty on the selection efficiency is demonstrated to be <0.3%.

3. Long-Baseline Neutrino Experiments

Long-baseline (LBL) experiments provide the only known practical way to measure the neutrino CP-violating phase (δ_{CP}). CP violation would manifest itself as a difference in the oscillation probability of $\nu_\alpha \to \nu_\beta$ between neutrinos and antineutrinos. The oscillation channel available for CP violation searches is electron (anti)neutrino appearance in a muon (anti)neutrino beam.

The oscillation probability of $\nu_\mu \to \nu_e$ through matter in the standard three-flavor model and a constant density approximation is, to first order [34]:

$$\begin{aligned} P(\overset{(-)}{\nu_\mu} \to \overset{(-)}{\nu_e}) \approx & \sin^2\theta_{23}\sin^2 2\theta_{13}\frac{\sin^2(\Delta_{31}-aL)}{(\Delta_{31}-aL)^2}\Delta_{31}^2 \\ & + \sin 2\theta_{23}\sin 2\theta_{13}\sin 2\theta_{12}\frac{\sin(\Delta_{31}-aL)}{(\Delta_{31}-aL)}\Delta_{31} \\ & \times \frac{\sin(aL)}{(aL)}\Delta_{21}\cos(\Delta_{31}\pm\delta_{CP}) \\ & + \cos^2\theta_{23}\sin^2 2\theta_{12}\frac{\sin^2(aL)}{(aL)^2}\Delta_{21}^2 \end{aligned}$$

where $a = \pm\, G_F\, N_e/\sqrt{2}$, G_F is the Fermi constant, N_e is the number density of electrons, and $\Delta_{ij} = 1.27\Delta m^2_{ij}L/E$, with L the baseline in km and E the neutrino energy in GeV. The first (last) term is the atmospheric (solar) probabilities and the middle term is the interference between the atmospheric and solar contributions. Both δ_{CP} and a terms are positive for $\nu_\mu \to \nu_e$ and negative for $\bar{\nu}_\mu \to \bar{\nu}_e$ oscillations.

Once a relatively large and non-zero θ_{13} was measured by reactor experiments, the measurement of the CP-violating phase is the main goal for the current generation of LBL experiments, T2K and NOvA. They are already providing valuable information about the CP-violating phase demonstrating that, in combination with reactor experiments, some values of δ_{CP} can already be excluded at 90% C.L. [15,35]. However, their sensitivity to δ_{CP} is limited and there is a general consensus in the community that more sensitive neutrino facilities will be necessary to make a definitive claim on the existence of CP violation. Two long-baseline neutrino projects are proposed: the DUNE experiment [36] in the US and the Hyper-Kamiokande experiment [37] in Japan. With different strategies and detector technologies, both DUNE and Hyper-K will have improved sensitivity to the CP-violating phase.

DUNE has a longer baseline length (1285 km) and higher neutrino beam energy (∼2.5 GeV) than Hyper-K (baseline = 295 km and neutrino peak energy ∼0.6 GeV). Therefore, DUNE is expected to be sensitive to the mass ordering while the baseline length of Hyper-K is too short for the matter effect that breaks the degeneracy so Hyper-K has poor sensitivity to the mass ordering. DUNE will decouple CP and matter effects by looking at the L/E dependence of ν_e and $\bar{\nu}_e$ appearance probabilities with a wide-band neutrino beam covering both the first and the second oscillation maxima. On the other hand, Hyper-K adopts the off-axis method to generate a low-energy narrow-band beam (<1 GeV) to compare the appearance of ν_e and $\bar{\nu}_e$ CC events at the first oscillation maximum.

Both DUNE and Hyper-K are sensitive to natural neutrino sources and will carry out a rich and complementary astroparticle physics program and they are massive enough to improve the search for the baryon number violation processes beyond current limits.

3.1. The DUNE Experiment

The Deep Underground Neutrino Experiment (DUNE) [38] is the next accelerator-based mega-science project after the LHC. DUNE has a very rich scientific program, starting from neutrino oscillations with the Fermilab Long-Baseline Neutrino Facility (LBNF) [39], and including nucleon decay searches, astroparticle physics (neutrinos from core-collapse supernovae [40] and solar neutrinos) and a wide range of BSM (Beyond the Standard Model) physics [41], as sterile neutrinos, non-standard interactions, and extra-dimensions.

DUNE (Figure 6) will observe neutrinos from the new LBNF neutrino beam (1.2 MW power upgradeable to 2.4 MW) originated at Fermi National Accelerator Laboratory (Fermilab), in Batavia, Illinois, USA. LBNF will use the high-power PIP-II [42] proton accelerator to produce a muon neutrino beam with a broad spectrum of neutrino energies that peaks at 2.5 GeV. Neutrinos will be measured by a near detector (ND) located at Fermilab just downstream of the beamline, and a far detector (FD), located 1285 km from the neutrino production point, at the Sanford Underground Research Facility (SURF), in Lead, South Dakota. The near detector [43] will consist of a suite of detector technologies designed to constrain systematic uncertainties in the oscillation measurements. The far detector (FD) will be a very large modular liquid argon time projection chamber (LArTPC) located 1840 m underground at SURF with a total mass of nearly 70 kt (fiducial mass of at least 40 kt) of liquid argon (LAr). This detector will be able to uniquely reconstruct neutrino interactions with millimeter precision and unprecedented resolution.

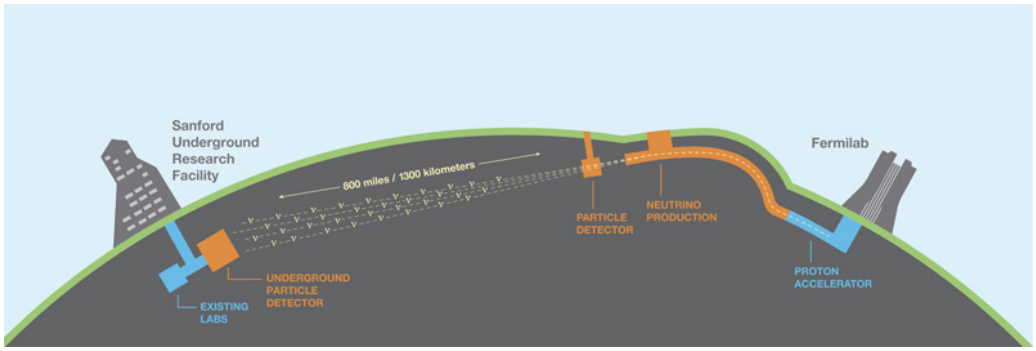

Figure 6. Cartoon illustrating the configuration of the LBNF beamline at Fermilab, in Illinois, and the DUNE detectors in Illinois and South Dakota, separated by 1300 km.

All these features and its capability to measure ν_μ disappearance and ν_e appearance will allow DUNE to unambiguously determine the neutrino mass ordering, discover charge-parity symmetry violation (CPV) in neutrinos for a wide range of possible values of the CP-violating phase δ_{CP}, and precisely measure δ_{CP}, θ_{13}, θ_{23}, and Δm^2_{32} in a single experiment. The neutrino and antineutrino-beam modes are critical to measure δ_{CP} and the mass ordering. These measurements will help guide the theory in understanding if there are new symmetries in the neutrino sector. The observation of CPV in neutrinos would be an important step in understanding the origin of the baryon asymmetry of the universe. The far detector technology and location deep underground will facilitate the study of low-energy neutrinos, including solar neutrinos and neutrinos from a core-collapse supernova, and searches for baryon number violating processes, such as proton decay and neutron-antineutron annihilation, and for other physics beyond the Standard Model.

The LArTPC technology has been selected for the DUNE FD because it combines fine-grained tracking with total absorption calorimetry to provide a detailed view of particle interactions. The precise imaging capability of the LArTPC FD allows one to identify and reconstruct signal events with high efficiency, while rejecting backgrounds, to provide a high-purity data sample. This feature and its high-energy resolution, together with the wide-band neutrino beam, enable the observation of several oscillation nodes, which is crucial for the measurement of three-flavor oscillation parameters in a single experiment.

The DUNE FD will be implemented as a set of four modules using independent cryostats, 65.8 m long by 17.8 m wide by 18.9 m high, each containing about 17.5 kt of LAr. Two detector modules will be located in each of the two caverns (see Figure 7). A central utility cavern will house electrical, HVAC, internet, cryogenics and other infrastructure for all the detector modules. A staged approach with the deployment of consecutive modules will enable an initial science program to begin early while allowing the implementation of improvements and developments of the far detector technology during the lifetime of the experiment.

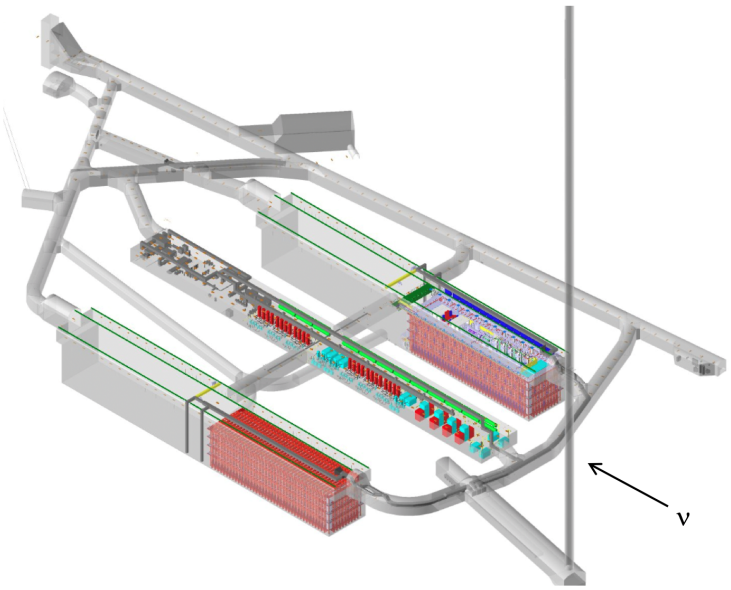

Figure 7. Underground caverns for the DUNE FD and cryogenics systems at SURF in South Dakota. The drawing shows the cryostats (red) for the first two FD modules. The vertical shaft providing access to the DUNE underground area appears on the right.

The first two FD modules differ in design. The first module uses horizontal drift technology (FD1-HD) [44], based on techniques used successfully by previous LArTPC detectors including ICARUS [45], MicroBooNE [46] and ProtoDUNE-SP [47]. In FD1-HD, ionization electrons from charged particles will drift horizontally under the influence of an electric field produced by vertically-oriented cathode and anode planes, with the active volume surrounded by a field-cage. The anode is formed by anode plane assemblies (APAs) that feature planes of thin wires wrapped around and soldered onto an insulating frame. Two wire planes acquire induced signals as the ionization electrons drift past them, and the third wire plane collects the ionization electrons. The photon detection system (PDS) is based on the X-ARAPUCA technology [48].

The second far detector module implements vertical drift technology (FD2-VD). This design features a horizontal cathode plane placed at mid-height in the active volume of the cryostat, dividing it into two vertically stacked equal volumes, each 6.5 m in height. The anode planes are constructed of perforated PCBs with etched electrodes forming a three-view charge readout. The top anode plane is placed close to the cryostat top, just below the surface of the LAr, and the other is located at the bottom of the cryostat. Ionization electrons will drift vertically towards the anode planes at the end of the drift volume in which they are released. The FD2-VD design offers a slightly larger instrumented volume (60.0 m $\times$ 13.5 m $\times$ 13.0 m) compared to the FD1-HD design and simpler, more cost-effective construction and installation due to its geometry. The FD2-VD design will implement the same X-ARAPUCA PDS technology as the FD1-HD design. The PDS is intended to provide an absolute initial time and interaction point location for neutrino charged-current events, a trigger for low-energy and supernova burst events and fiducialization of baryon number-violating nucleon decays.

3.2. Long-Baseline Neutrino Oscillation Physics in DUNE

The study of the oscillation patterns of high-intensity ν_μ and $\bar{\nu}_\mu$ beams over a baseline of ∼1300 km in DUNE will permit a detailed study of neutrino mixing, definitive resolution of the neutrino mass ordering, and a sensitive search for charge-parity symmetry violation (CPV) in the lepton sector in a single experiment [39].

The expected FD $\nu_\mu \rightarrow \nu_e$ and $\nu_\mu \rightarrow \nu_\mu$ event rates are shown in Figures 8 and 9 for an exposure of 336 kt-MW-years (seven years of operation assuming a staging scenario of detector modules operation and beam upgrade [39]).

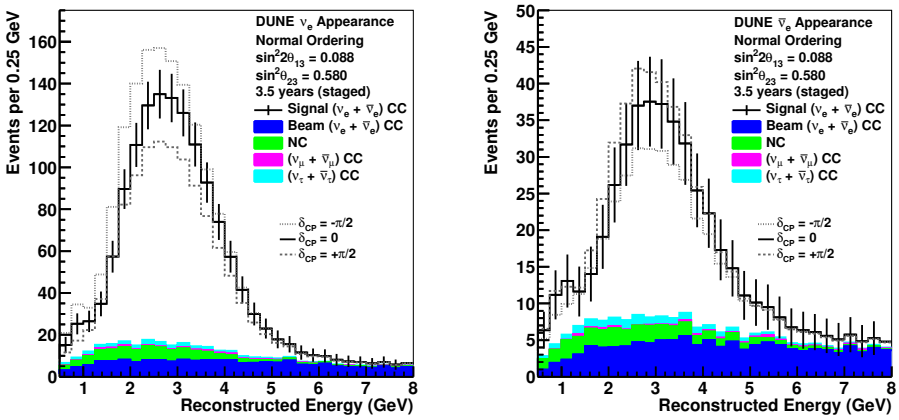

Figure 8. ν_e and $\bar{\nu}_e$ appearance spectra: reconstructed energy distribution of selected ν_e CC-like events assuming 336 kt-MW-years exposure, with equal running in the neutrino and antineutrino-beam mode. Statistical uncertainties are shown on the datapoints. The plots assume normal mass ordering and include curves for $\delta_{CP} = -\pi/2, 0$, and $\pi/2$ [39].

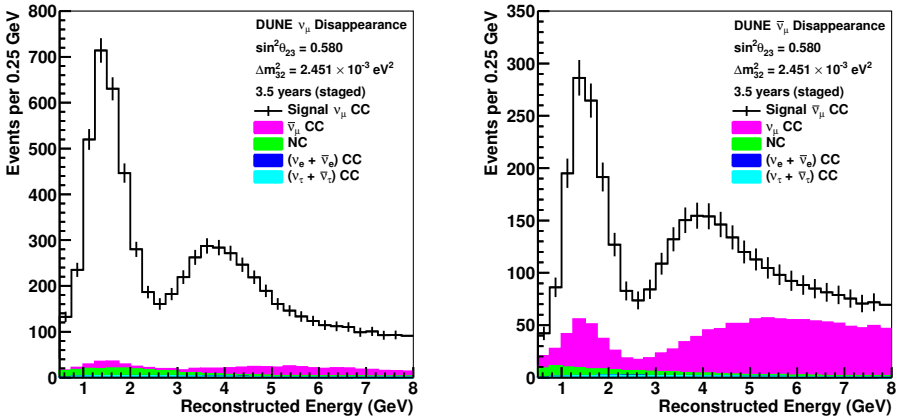

Figure 9. ν_μ and $\bar{\nu}_\mu$ disappearance spectra: reconstructed energy distribution of selected ν_μ CC-like events assuming assuming 336 kt-MW-years exposure, with equal running in the neutrino and antineutrino-beam mode. Statistical uncertainties are shown on the datapoints. The plots assume normal mass ordering [39].

DUNE sensitivities to oscillation parameters are derived from simultaneous likelihood fits to the four far detector samples (ν_μ disappearance and ν_e appearance for both neutrino and antineutrino beams) plus additional near detector samples. Systematic uncertainties from the neutrino flux model, the neutrino cross section model, detector effects, and unmeasured oscillation parameters are included in the fits, as described in [39,49]. The resulting sensitivities to CPV, and mass ordering at different times during the experiment's operation are shown in Figure 10. DUNE will be able to establish the neutrino mass ordering at the 5σ level for 100% of δ_{CP} values between two and three years. CP violation can be observed with 5σ significance after ∼7 years if $\delta_{CP} = -\pi/2$ and after ∼10 years for

50% of δ_{CP} values. CP violation can be observed with 3σ significance for 75% of δ_{CP} values after ~13 years of running.

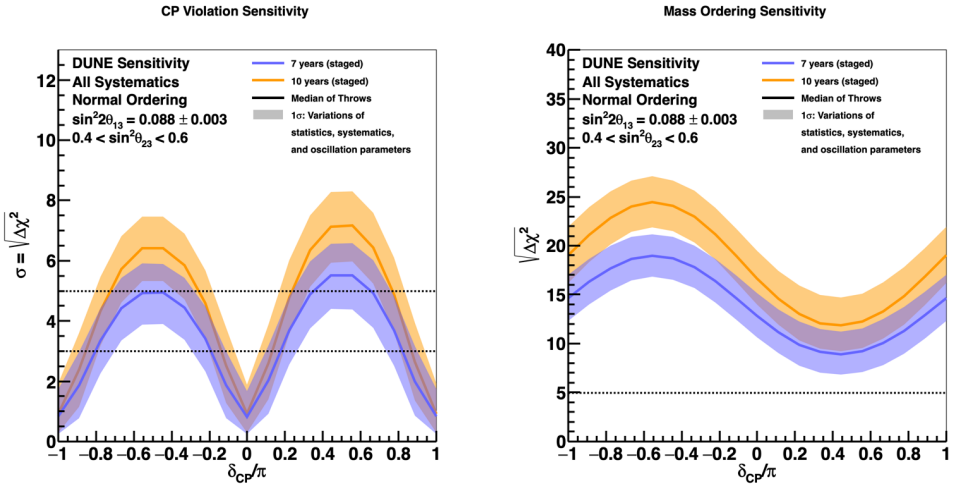

Figure 10. (**Left**): Significance of the DUNE determination of CPV ($\delta_{CP} \neq [0, \pm\pi]$) as a function of the true value of δ_{CP}, for seven (blue) and ten (orange) years of exposure, in normal ordering. (**Right**): Significance of the DUNE determination of the neutrino mass ordering, as a function of the true value of δ_{CP}, for seven (blue) and ten (orange) years of exposure, in normal ordering. The width of the transparent bands cover 68% of fits in which random throws are used to simulate systematic, oscillation parameter and statistical variations, with independent fits performed for each throw constrained by prior uncertainties. The solid lines show the median significance [39].

Figure 11 shows the resolution, in degrees, of DUNE's measurement of δ_{CP}, as a function of the true value of δ_{CP}, for true normal ordering. For 15 years of exposure, the δ_{CP} resolution between five and fifteen degrees are possible, depending on the true δ_{CP} value.

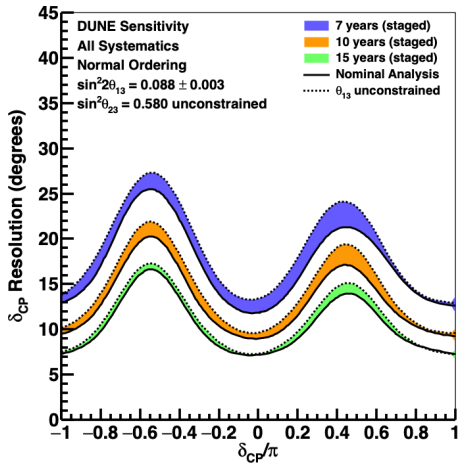

Figure 11. Resolution in degrees for the DUNE measurement of δ_{CP}, as a function of the true value of δ_{CP}, for seven (blue), ten (orange), and fifteen (green) years of exposure. The width of the band shows the impact of applying an external constraint on θ_{13} [39].

The expected DUNE measurement of $\sin^2 2\theta_{13}$ will approach the precision of reactor experiments for high exposure, allowing measurements that do not rely on an external $\sin^2 2\theta_{13}$ constraint and facilitating a comparison between the DUNE and reactor $\sin^2 2\theta_{13}$ results, which is of interest as a potential signature for physics beyond the standard model. In addition, DUNE will have significant sensitivity to the θ_{23} octant for values of $\sin^2 2\theta_{23}$ less than about 0.47 and greater than about 0.55.

The measurements made by DUNE will significantly advance our understanding of the standard three-flavor mixing picture and will provide invaluable inputs to continuing work toward understanding flavor, potential new symmetries reflected in the neutrino sector, and the relationship between the generational structure of quarks and leptons. The observation of CPV in neutrinos would be an important step in understanding the origin of the baryon asymmetry of the universe. The precise measurements of the three-flavor mixing parameters that DUNE will provide may also yield inconsistencies that point us to physics beyond the standard three-flavor model.

3.3. The ProtoDUNE Program at CERN

The DUNE collaboration has constructed and operated two large prototype detectors, each with an active mass of about 400 t, ProtoDUNE-SP, and ProtoDUNE-DP, at the CERN Neutrino Platform (Figure 12), with the aim of validating the LArTPC technology for DUNE at large scale and measuring the detector response to different particles from a test beam.

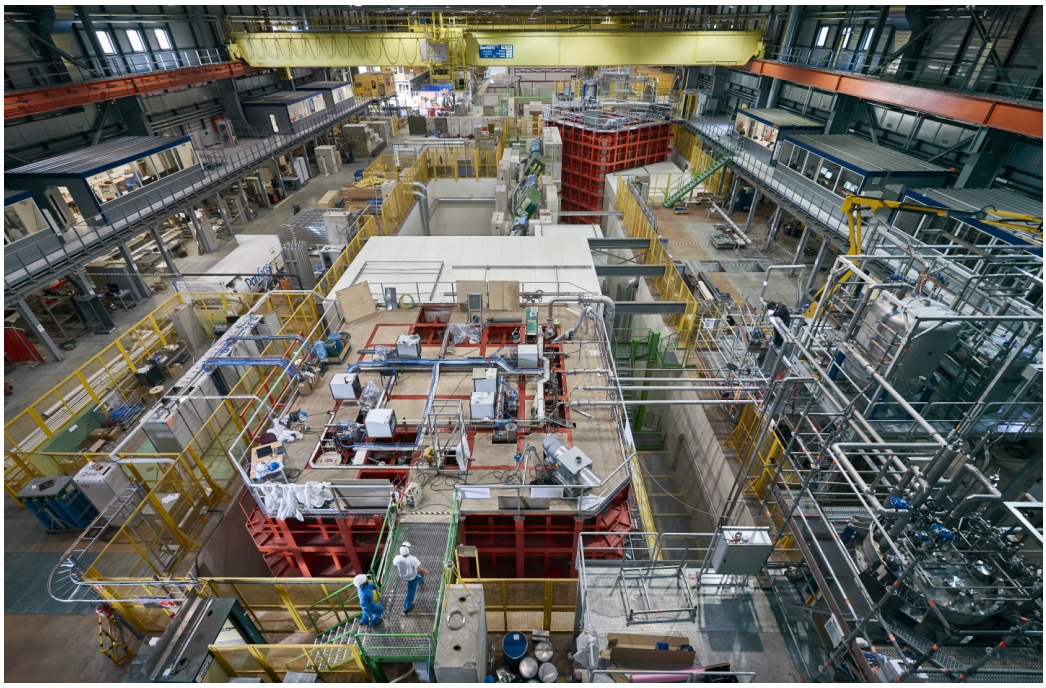

Figure 12. ProtoDUNE-SP (in the foreground) and ProtoDUNE-DP (in the background) installed at the CERN Neutrino Platform. Image: CERN.

Each prototype is approximately one-twentieth the size of each of the planned FD modules but uses components identical in size to those of the full-scale module. The main difference between them is the readout process of the ionization charge produced in the interactions in the LAr. In ProtoDUNE-SP, the ionization electrons drift horizontally towards the anode planes submerged in the LAr, where they induce electrical signals; in DP, the electrons are extracted from the liquid to a thin gas phase where they are amplified and collected on readout anodes. Figure 13 shows the inner volume of ProtoDUNE-SP on the left and the single drift volume of ProtoDUNE-DP on the right.

The ProtoDUNE-SP detector [47], with a total LAr mass of 0.77 kt, is the largest LArTPC operated to date. ProtoDUNE-SP is a prototype for the first DUNE FD module and it incorporates full size components as designed for that module. The volume is segmented in two parts, with two anode planes on the sides and a central cathode, having a maximum drift length of 3.6 m. ProtoDUNE-SP collected charged-particle test beam and cosmic ray data from 2018 to 2021 [50].

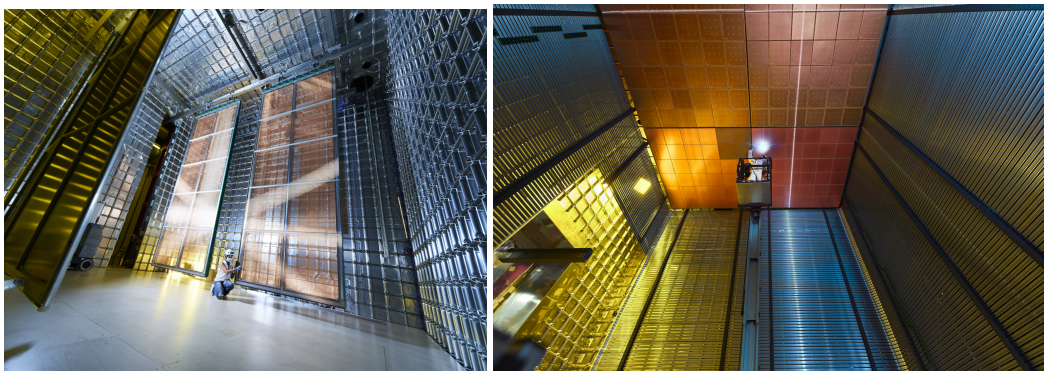

Figure 13. (**Left**): Inner view of ProtoDUNE-SP. (**Right**): Drift volume of ProtoDUNE-DP. Image: CERN.

ProtoDUNE-SP has successfully implemented the LArTPC technology in a scalable design demonstrating its suitability for a single-phase DUNE Far Detector module. ProtoDUNE-SP data (Figure 14) exhibits superb detector performance and signal to noise ratio. A new prototyping phase, including detector upgrades and additional test-beam data, is scheduled to start at CERN in 2022.

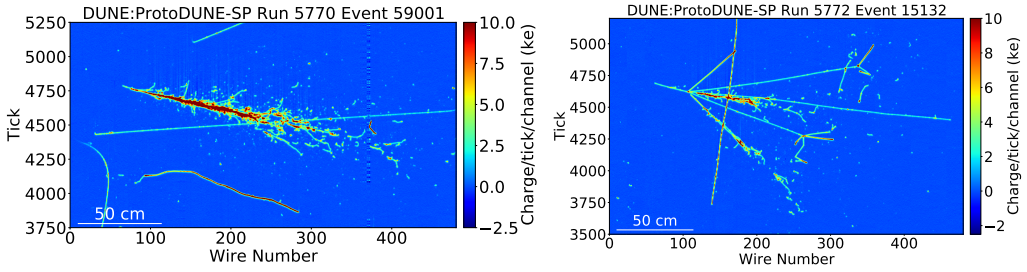

Figure 14. (**Left**): A 6 GeV/c electron candidate. (**Right**): A 6 GeV/c pion candidate [50].

The ProtoDUNE Dual Phase (ProtoDUNE-DP) [51] detector was operated from 2019 to 2020 at the CERN Neutrino Platform to demonstrate the LArTPC DP technology at large scale. ProtoDUNE-DP has an active volume of $6 \times 6 \times 6$ m^3 corresponding to an active mass of 300 t (total LAr mass of 750 t), being the largest DP LArTPC ever operated. In ProtoDUNE-DP the electric drift field is oriented in the vertical direction, causing the electrons to drift vertically towards the anode at the top. The ionization charge is then extracted, amplified, and detected in gaseous argon above the liquid surface by the charge readout planes. The scintillation light signal is collected by a photon detection system (PDS) [52] constructed out of photo-multiplier tubes (PMTs).

Although the DP technology proved challenging in some aspects, it has provided valuable knowledge that informs the VD design described earlier. The detector will be refurbished in 2023 with the goal of validating the vertical drift (VD) design at a large scale and testing its long-term stability.

3.4. Spanish Contribution to DUNE

DUNE is an international collaboration of 1435 members from 228 institutions in 38 countries (50% US- 50% non-US), including CERN and Spain. It is, by far, the largest scientific collaboration devoted to neutrino physics to date. Spain currently represents ∼4% of the total DUNE membership.

The DUNE research program is considered a priority in both Europe and the United States. According to the 2020 Update of the European Strategy for Particle Physics [53] that will guide the future of particle physics in Europe, approved by the CERN Council on 19 June 2020: "Europe, and CERN through the Neutrino Platform, should continue to support long baseline experiments in Japan and the United States. In particular, they

should continue to collaborate with the United States and other international partners towards the successful implementation of the Long-Baseline Neutrino Facility (LBNF) and the Deep Underground Neutrino Experiment (DUNE)".

The Spanish groups are members of DUNE since its foundations in 2015. They are heavily involved in the DUNE R&D phase, being responsible for important systems of the ProtoDUNE detectors at the CERN Neutrino Platform. The photon detection system is a crucial element in the LArTPC technology, since the primary scintillation light recorded by this system provides the event time information, and contributes to the triggering and to the reconstruction of the events. The Spanish groups, in a coordinated way, have led the construction and operation of the photon detection system of ProtoDUNE-DP and are also contributing to the upgrades for the next ProtoDUNE phase at CERN.

CIEMAT, together with IFAE, has been responsible for the photon detection system of ProtoDUNE-DP, including the acquisition and characterization of 40 8" cryogenic photomultipliers [54], coating with wavelength shifters, design and production of the voltage circuit and HV splitters, production of the associated mechanics [55], light calibration system [56], readout and data acquisition systems [57], and final installation and commissioning of the light detection system in the detector. Figure 15 shows the ProtoDUNE-DP PMTs installed at the bottom of the ProtoDUNE-DP cryostat.

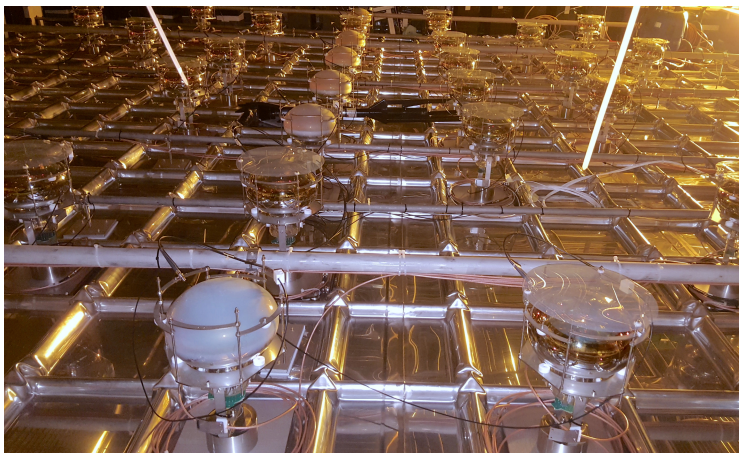

Figure 15. ProtoDUNE-DP PDS formed of 36 PMTs installed at the bottom of the cryostat at CERN.

Spanish groups have developed the simulation of the ProtoDUNE-DP PDS and scintillation light processes and are the leaders of the analysis of the scintillation light data [58]. The photon detection system collected cosmic-ray data for 18 months in stable conditions with all 36 PMTs operative. The good performance of the system has validated the design for use in future long drift distance LArTPCs. The size of ProtoDUNE-DP, the longest drift-distance LArTPC ever operated, has allowed for an unprecedented study of the light propagation. ProtoDUNE-DP data has also demonstrated the improvement of the light detection efficiency and uniformity in large LArTPCs due to Xe doping.

In addition to the PDS, the Spanish groups are also involved in the temperature monitoring system. This is a mandatory element to guarantee the detector performance providing a 3D temperature map over the entire cryostat with a precision better than 0.005 K. This system was also built in Spain for ProtoDUNE-SP.

The analysis of the acquired ProtoDUNE data at CERN is being performed by the Spanish PhD students as part of their theses [59,60]. Computing resources from Spanish institutions are being used for ProtoDUNE data processing and simulation production. Spanish group members are also very active in preparing the DUNE physics program and analysis tools, and are among the main authors of the latest DUNE publications.

Spain is one of the main contributors to the DUNE FD photon detection system, being in charge, together with some European partners, of the design, construction and test of critical elements of the system, as the SiPM sensors, dichroic filters, wavelength-shifting

bars, and electronics, that make up the X-ARAPUCAs. Many components of the system are being developed, assembled and tested in the Spanish laboratories. The temperature monitoring system for the first two FD modules is also being built in Spain. In addition, Spain contributes to the DUNE data storage and data processing with dedicated resources. Other opportunities of participation in the DUNE near detectors and third and fourth FD modules are being explored by the Spanish institutions.

4. Conclusions

The complementarity between accelerator and reactor neutrino experiments and their different approaches to measure the neutrino oscillations has allowed to establish precise constraints for three-flavor neutrino oscillations. Measurements with different sources of neutrinos at very different energies and baselines has proved essential in the understanding of the neutrino oscillation phenomenon. The measurement of the still unknown δ_{CP}, θ_{23} octant and mass ordering parameters in the followingw years is only possible thanks to the interplay between the reactor and accelerator neutrino experiments.

Reactor neutrino experiments, and in particular Double Chooz, have provided a precise measurement of the θ_{13} mixing angle. Unlike accelerator neutrino experiments, the reactor measurements are independent of the CP phase and θ_{23}, and only slightly dependent on the neutrino mass ordering and matter effect. On the other hand, long-baseline neutrino experiments with accelerators can study both ν_μ disappearance and ν_e appearance modes from a ν_μ beam, having access to the measurement of crucial oscillation parameters, in particular the CP violation in the lepton sector. The DUNE experiment will combine the world's most intense neutrino beam, a deep underground site, and massive LAr detectors to enable a broad science program addressing some of the most fundamental questions in particle physics.

Spain has played a crucial role in the recent neutrino oscillation results, in particular, the discovery of the θ_{13} mixing angle by the Double Chooz experiment, and will continue to strongly contribute to the LArTPC ProtoDUNE program at CERN and to the DUNE long-baseline neutrino experiment at Fermilab.

Author Contributions: Investigation, I.G.-B., C.P.; writing—original draft preparation, I.G.-B., C.P.; writing—review and editing, I.G.-B., C.P. All authors have read and agreed to the published version of the manuscript.

Funding: This work is supported by the Spanish Ministry of Science and Innovation under Grant no. PID2019-104676GB-C31.

Institutional Review Board Statement: Not applicable.

Informed Consent Statement: Not applicable.

Data Availability Statement: Not applicable.

Acknowledgments: We thank Double Chooz and DUNE collaborations for the material presented in this review. We are grateful to José Ignacio Crespo-Anadón and Clara Cuesta for their careful reading of the manuscript.

Conflicts of Interest: The authors declare no conflict of interest.

References

1. De Salas, P.F.; Forero, D.V.; Gariazzo, S.; Martínez-Miravé, P.; Mena, O.; Ternes, C.A.; Tórtola, M.; Valle, J.W.F. 2020 global reassessment of the neutrino oscillation picture. *J. High Energy Phys.* **2021**, *02*, 071. [CrossRef]
2. Von Feilitzsch, F.; Hahn, A.A.; Schreckenbach, K. Experimental beta spectra from Pu-239 and U-235 thermal neutron fission products and their correlated anti-neutrinos spectra. *Phys. Lett. B* **1982**, *118*, 162–166. [CrossRef]
3. Schreckenbach, K.; Colvin, G.; Gelletly, W.; Von Feilitzsch, F. Determination of the anti-neutrino spectrum from U-235 thermal neutron fission products up to 9.5 MeV. *Phys. Lett. B* **1985**, *160*, 325–330. [CrossRef]
4. Mueller, T.A.; Lhuillier, D.; Fallot, M.; Letourneau, A.; Cormon, S.; Fechner, M.; Giot, L.; Lasserre, T.; Martino, J.; Mention, G.; et al. Improved Predictions of Reactor Antineutrino Spectra. *Phys. Rev. C* **2011**, *83*, 054615. [CrossRef]

5. Haag, N.; Guetlein, A.; Hofmann, M.; Oberauer, L.; Potzel, W.; Schreckenbach, K.; Wagner, F.M. Experimental Determination of the Antineutrino Spectrum of the Fission Products of ^{238}U. *Phys. Rev. Lett.* **2014**, *112*, 122501. [CrossRef]
6. Huber, P. On the determination of anti-neutrino spectra from nuclear reactors. *Phys. Rev. C* **2011**, *84*, 024617. [CrossRef]
7. Eguchi, K.; Enomoto, S.; Furuno, K.; Goldman, J.; Hanada, H.; Ikeda, H.; Ikeda, K.; Inoue, K.; Ishihara, K.; Itoh, W.; et al. First results from KamLAND: Evidence for reactor anti-neutrino disappearance. *Phys. Rev. Lett.* **2003**, *90*, 021802. [CrossRef]
8. Ardellier, F.; Barabanov, I.; Barriere, J.C.; Beißel, F.; Berridge, S.; Bezrukov, L.; Bernstein, A.; Bolton, T.; Bowden, N.S.; Buck, C.; et al. Double Chooz, A Search for the Neutrino Mixing Angle theta-13. *arXiv* **2006**, arXiv:hep-ex/0606025.
9. Daya Bay Collaboration. A Precision Measurement of the Neutrino Mixing Angle theta-13 using Reactor Antineutrinos at Daya Bay. *arXiv* **2007**, arXiv:hep-ex/0701029.
10. RENO Collaboration. RENO: An Experiment for Neutrino Oscillation Parameter theta-13 Using Reactor Neutrinos at Yonggwang. *arXiv* **2010**, arXiv:1003.1391.
11. Double Chooz Collaboration. Indication of Reactor $\bar{\nu}_e$ Disappearance in the Double Chooz Experiment *Phys. Rev. Lett.* **2012**, *108*, 131801. [CrossRef]
12. Double Chooz Collaboration. Reactor electron antineutrino disappearance in the Double Chooz experiment. *Phys. Rev. D* **2012**, *86*, 052008. [CrossRef]
13. Double Chooz Collaboration. Improved measurements of the neutrino mixing angle θ_{13} with the Double Chooz detector. *J. High Energy Phys.* **2014**, *10*, 086.
14. Double Chooz Collaboration. Double Chooz θ_{13} measurement via total neutron capture detection. *Nat. Phys.* **2020**, *16*, 558–564. [CrossRef]
15. T2K Collaboration. Improved constraints on neutrino mixing from the T2K experiment with 3.13×10^{21} protons on target *Phys. Rev. D* **2021**, *103*, 112008. [CrossRef]
16. NOvA Collaboration. New constraints on oscillation parameters from ν_e appearance and ν_μ disappearance in the NOvA experiment *Phys. Rev. D* **2018**, *98*, 032012. [CrossRef]
17. Daya Bay Collaboration. Measurement of the Electron Antineutrino Oscillation with 1958 Days of Operation at Daya Bay. *Phys. Rev. Lett.* **2018**, *121*, 241805. [CrossRef]
18. RENO Collaboration. Measurement of Reactor Antineutrino Oscillation Amplitude and Frequency at RENO. *Phys. Rev. Lett.* **2018**, *121*, 201801. [CrossRef]
19. Cucoanes, A.; Novella, P.; Cabrera, A.; Fallot, M.; Onillon, A.; Obolensky, M.; Yermia, F. Reactor Neutrino Flux Uncertainty Suppression on Multiple Detector Experiments. *arXiv* **2015**, arXiv:1501.00356.
20. Hiraide, K.; Minakata, H.; Nakaya, T.; Nunokawa, H.; Sugiyama, H.; Teves, W.J.; Funchal, R.Z. Resolving θ_{23} degeneracy by accelerator and reactor neutrino oscillation experiments. *Phys. Rev. D* **2006**, *73*, 093008. [CrossRef]
21. Berryman, J.; Brdar, V.; Huber, P. Particle physics origin of the 5 MeV bump in the reactor antineutrino spectrum? *Phys. Rev. D* **2019**, *99*, 055045. [CrossRef]
22. Daya Bay Collaboration. Improved Measurement of the Reactor Antineutrino Flux and Spectrum at Daya Bay. *Chin. Phys. C* **2017**, *41*, 013002. [CrossRef]
23. RENO Collaboration. Observation of Reactor Electron Antineutrino Disappearance in the RENO Experiment. *Phys. Rev. Lett.* **2012**, *108*, 191802. [CrossRef]
24. NEOS Collaboration. Sterile Neutrino Search at the NEOS Experiment *Phys. Rev. Lett.* **2017**, *118*, 121802. [CrossRef]
25. Calvo, E.; Cerrada, M.; Fernandez-Bedoya, C.; Gil-Botella, I.; Palomares, C.; Rodríguez, I.; Toral, F.; Verdugo, A. Characterization of large area photomutipliers under low magnetic fields: Design and performances of the magnetic shielding for the Double Chooz neutrino experiment. *Nucl. Instrum. Meth. A* **2010**, *621*, 222–230. [CrossRef]
26. Calvo, E.; Cerrada, M.; Gil-Botella, I.; Palomares, C.; Rodriguez, I.; Toral, F.; Verdugo, A. Passive magnetic cylindrical shielding at gauss-range static fields. *Nucl. Instrum. Meth. A* **2009**, *600*, 560–567. [CrossRef]
27. Double Chooz Collaboration. Characterization of the Spontaneous Light Emission of the PMTs used in the Double Chooz Experiment. *J. Instrum.* **2016**, *11*, 08001.
28. Double Chooz Collaboration. Background-independent measurement of θ_{13} in Double Chooz. *Phys. Lett. B* **2014**, *735*, 51–56. [CrossRef]
29. Double Chooz Collaboration. Measurement of θ_{13} in Double Chooz using neutron captures on hydrogen with novel background rejection techniques. *J. High Energy Phys.* **2016**, *01*, 163.
30. Double Chooz Collaboration. Reactor rate modulation oscillation analysis with two detectors in Double Chooz. *J. High Energy Phys.* **2021**, *01*, 190.
31. López-Castaño, J.M. Evaluación e impacto del fondo en la medida del ángulo de mezcla θ_{13} en el experimento Double Chooz. Ph.D. Thesis, Universidad Complutense de Madrid, Madrid, Spain, 1 December 2017.
32. Crespo-Anadón, J.I. Measurement of the Neutrino Mixing Angle θ_{13} in the Double Chooz Experiment. Ph.D. Thesis, Universidad Complutense de Madrid, Madrid, Spain, 30 November 2015.
33. Navas-Nicolás, D. Measurement of the θ_{13} Neutrino Mixing Angle with the Two Detectors of the Double Chooz Experiment. Ph.D. Thesis, Universidad Complutense de Madrid, Madrid, Spain, 27 May 2019.
34. Nunokawa, H.; Parke, S.J.; Valle, J.W.F. CP Violation and Neutrino Oscillations. *Prog. Part. Nucl. Phys.* **2008**, *60*, 338–402. [CrossRef]

35. NOvA Collaboration. An Improved Measurement of Neutrino Oscillation Parameters by the NOvA Experiment. *arXiv* **2021**, arXiv:2108.08219.
36. DUNE Collaboration. Long-Baseline Neutrino Facility (LBNF) and Deep Underground Neutrino Experiment (DUNE): Conceptual Design Report, Volume 1: The LBNF and DUNE Projects. *arXiv* **2016**, arXiv:1601.05471.
37. Hyper-Kamiokande Collaboration. Hyper-Kamiokande Design Report. *arXiv* **2018**, arXiv:1805.04163.
38. DUNE Collaboration. Deep Underground Neutrino Experiment (DUNE), Far Detector Technical Design Report, Volume I Introduction to DUNE. *J. Instrum.* **2020**, *15*, T08008.
39. DUNE Collaboration. Long-baseline neutrino oscillation physics potential of the DUNE experiment. *Eur. Phys. J. C* **2020**, *80*, 978. [CrossRef]
40. DUNE Collaboration. Supernova neutrino burst detection with the Deep Underground Neutrino Experiment. *Eur. Phys. J. C* **2021**, *81*, 423. [CrossRef]
41. DUNE Collaboration. Prospects for beyond the Standard Model physics searches at the Deep Underground Neutrino Experiment. *Eur. Phys. J. C* **2021**, *81*, 322. [CrossRef]
42. Valeri, L. *The PIP-II Reference Design Report*; U.S. Department of Energy: Germantown, MD, USA, 2015. [CrossRef]
43. DUNE Collaboration. Deep Underground Neutrino Experiment (DUNE) Near Detector Conceptual Design Report. *Instruments* **2021**, *5*, 31. [CrossRef]
44. DUNE Collaboration. Deep Underground Neutrino Experiment (DUNE), Far Detector Technical Design Report, Volume IV: Far Detector Single-phase Technology. *J. Instrum.* **2020**, *15*, T08010. [CrossRef]
45. ICARUS Collaboration. Design, construction and tests of the ICARUS T600 detector. *Nucl. Instrum. Meth. A* **2004**, *527*, 329–410. [CrossRef]
46. MicroBooNE Collaboration. Design and Construction of the MicroBooNE Detector. *J. Instrum.* **2017**, *12*, P02017. [CrossRef]
47. DUNE Collaboration. Design, construction and operation of the ProtoDUNE-SP Liquid Argon TPC. *arXiv* **2021**, arXiv:2108.01902.
48. Machado, A.A.; Segreto, E. ARAPUCA a new device for liquid argon scintillation light detection. *J. Instrum.* **2016**, *11*, C02004. [CrossRef]
49. DUNE Collaboration. Deep Underground Neutrino Experiment (DUNE), Far Detector Technical Design Report, Volume II: DUNE Physics. *arXiv* **2020**, arXiv:2002.03005.
50. DUNE Collaboration. First results on ProtoDUNE-SP liquid argon time projection chamber performance from a beam test at the CERN Neutrino Platform. *J. Instrum.* **2020**, *15*, P12004. [CrossRef]
51. De Bonis, I.; Del Amo Sanchez, P.; Duchesneau, D.; Pessard, H.; Bordoni, S.; Ieva, M.; Lux, Y.; Sanchez, F.; Jipa, A.; Lazanu, I.; et al. LBNO-DEMO: Large-scale neutrino detector demonstrators for phased performance assessment in view of a long-baseline oscillation experiment. *arXiv* **2014**, arXiv:1409.4405.
52. DUNE Collaboration. Photon detection system for ProtoDUNE dual phase. *J. Instrum.* **2017**, *12*, C12048. [CrossRef]
53. 2020 Update of the European Strategy for Particle Physics. CERN-ESU-015. 2020. Available online: https://cds.cern.ch/record/2721370 (accessed on 20 January 2022).
54. Belver, D.; Calvo, E.; Cuesta, C.; Gallego-Ros, A.; Gil-Botella, I.; Jiménez, S.; Lastoria, C.; Lux, T.; Palomares, C.; Redondo, D.; et al. Cryogenic R5912-20Mod Photomultiplier Tube Characterization for the ProtoDUNE Dual Phase Detector. *J. Instrum.* **2018**, *13*, T10006. [CrossRef]
55. Belver, D.; Calvo, E.; Cuesta, C.; Gallego-Ros, A.; Gil-Botella, I.; Jiménez, S.; Lastoria, C.; Martín, I.; Martínez, J.J.; Palomares, C.; et al. First testing of the Hamamatsu R5912-02Mod photomultiplier tube at 4-bar pressure and cryogenic temperature. *J. Instrum.* **2020**, *15*, P09023. [CrossRef]
56. Belver, D.; Boix, J.; Calvo, E.; Cuesta, C.; Gallego-Ros, A.; Gil-Botella, I.; Jiménez, S.; Lastoria, C.; Lux, T.; Martín, I.; et al. A Light Calibration System for the ProtoDUNE-DP Detector. *J. Instrum.* **2019**, *14*, T04001. [CrossRef]
57. Belver, D.; Boix, J.; Calvo, E.; Cuesta, C.; Gallego-Ros, A.; Gil-Botella, I.; Jiménez, S.; Lastoria, C.; Lux, T.; Martín, I.; et al. ProtoDUNE-DP Light Acquisition and Calibration Software. *IEEE Trans. Nucl. Sci.* **2021**, *68*, 2334–2341. [CrossRef]
58. DUNE Collaboration. Scintillation light detection in the 6-m drift length ProtoDUNE Dual Phase liquid argon TPC. *arXiv* **2021**, arXiv:2110.15007.
59. Lastoria, C. Analysis of the Scintillation Light Production and Propagation in the WA105 Dual-Phase Demonstrator. Ph.D. Thesis, Universidad Complutense de Madrid, Madrid, Spain, 17 December 2020.
60. Gallego-Ros, A. Studies on the Scintillation Light Detection in the ProtoDUNE Dual Phase Liquid-Argon TPC and Its Capability for the Supernova Trigger in DUNE. Ph.D. Thesis, Universidad Autónoma de Madrid, Madrid, Spain, 15 December 2021.